

Supporting Information

Ma et al. 10.1073/pnas.1001065107

SI Materials and Methods

Cell Lines, Transfections, and in Vitro Tumorigenic Assays. Primary human dermal microvascular endothelial cells (HMVEC) were obtained from Lonza and cultured in EGM-2 medium (Lonza). Immortalized human dermal microvascular endothelial cells (HMEC1) were obtained from the CDC and grown in Gibco MCDB 131 medium (Invitrogen), supplemented with 10% FBS, 10 mM/L-glutamine, 10 ng/mL epidermal growth factor, 1 μ g/mL hydrocortisone, and 1% antibiotic antimycotic. Immortalized murine endothelial cells (SVEC) and SVEC stable cell lines expressing KSHV vGPCR or KSHV vCyc and vFlip are described in ref. 1. shRNA cell lines were generated using pSilencer 2.1-U6 puro vector (Applied Biosystems). Hairpin sequences are as follows: ANGPTL4 (two selected clones; 1 and 2) (sense 5'-GATCCAGAAGCTTTCCAAGATGACTTCAAGAGAGTCATCTTGGAAGCTTCTTTTTTTGGAAA-3'; and antisense 5'-AGCTTTTCCAAAAAAGAAGCTTTCCAAGATGACTCTCTTGAAGTCATCTTGGAAAGCTTCTG-3'). DNA and siRNA delivery to cells was performed using PolyFect (Qiagen) or HiPerFect (Qiagen), respectively. BrdU incorporation assays and colony growth in soft agar was determined as described in ref. 1.

Western Blot, Immunohistochemistry, and Microscopy. Western blot, immunohistochemistry, and indirect immunofluorescence were performed as described in ref. 1. Antibodies were obtained as follows: ANGPTL4 from Chemicon, ZO1 from Zymed, β -catenin and α -tubulin from Santa Cruz, AU5 from Covance, P-Akt from Cell Signaling, Akt from R&D Systems, and CD31 from BD PharMingen. Polyclonal vGPCR antibody was kindly provided by Gary S. Hayward (Johns Hopkins University, Baltimore, MD) (2). Confocal microscopy was performed using a Zeiss LSM 510 Meta microscope. H&E stainings of the vGPCR experimental and human KS tumors were scanned at 200 \times using an Aperio T3 Scanscope.

Animal Studies. All procedures involving animals were approved by the Institutional Animal Care and Use Committee. vGPCR experimental tumors were obtained as described in ref. 1. Briefly, *TIE2-tva* transgenic mice expressing in vascular endothelium the avian leukosis virus (ALV) receptor, TVA, were injected i.p. with ALV-derived retrovirus encoding for KSHV vGPCR. Macroscopic vGPCR tumors developed in 4 mo, predominantly in tail, paws, and GI tract. For allograft formation, early passage, exponentially growing cells were injected s.c. in the right flank of 8-wk-old athymic (*nu/nu*) nude female mice. The animals were monitored twice weekly for tumor formation. Tumors' longest length (L) and shortest width (W) were measured using a caliper at different time points throughout the experiment. Tumor volume was then converted into tumor weight using the formula $LW^2/2$. When appropriate, animals were euthanized, and tissue was fixed in 4% paraformaldehyde and embedded in paraffin for further analysis. vGPCR and vGPCR/TK allografts were described in ref. 3. Treatment of established (50–100 mg) vGPCR/TK tumors with ganciclovir (50 mg/kg) for 6 consecutive d leads to complete loss of all vGPCR-expressing cells in the tumor. For vCyc/vFlip + vGPCR allografts, 10^5 vGPCR-expressing cells were mixed with 10^6 vCyc/vFlip-expressing cells, following the (1:10) ratio of expressing cells in human KS (4), and injected s.c. into the flank of nude mice (3).

qRT-PCR. Total RNA was isolated using the GenElute Mammalian Total RNA Miniprep Kit (Sigma), and reverse transcription was performed using SuperScript III First-Strand Synthesis System

(Invitrogen). qRT-PCR was performed on a 96-well/plate ABI7-000HT machine (2 min at 50 $^{\circ}$ C, 10 min at 95 $^{\circ}$ C, and 40 cycles of 15 s at 94 $^{\circ}$ C and 1 min at 60 $^{\circ}$ C) using SYBR Green Master-Mix (Applied Biosystems). Primers for human Angptl4 were 5'-CGTGGGGACCTTAACTGTG-3' (sense) and 5'-TTCCATG-TTTTCCAGAAGATAC-3' (antisense). GAPDH was used for normalization.

In Vitro Endothelial Cell Migration and Tube Formation (Matrigel) Assays. For (inverse) cell migration, serum-starved 2×10^4 /well HMECs were plated in the bottom wells of a Boyden chamber, and a fibronectin-coated polycarbonate membrane (8 μ m; Neuroprobe, Inc.) was placed above. The chamber was inverted and incubated for 2 h at 37 $^{\circ}$ C to allow cell attachment. Fifty milliliters of chemotactic sample was added to the top wells. After 6 h, the membrane was stained with Diff-Quick stain (Dade Behring) and analyzed with ImageJ 1.41 (<http://rsbweb.nih.gov/ij/index.html>). For tube formation, 100 μ L of growth factor-free matrigel was polymerized in 96-well plates. HMEC (2×10^4 /well) in 50 μ L of 2% FBS MCDB 131 medium were mixed with 50 μ L of test sample and added onto the matrigel surface. Eighteen hours later, capillary-like tubule formation was labeled with BD Calcein AM (Becton Dickinson). Digital images were obtained using a video camera system. Total tube length was determined using ImageJ 1.41.

Directed in Vivo Angiogenesis Assay (DIVAA). The DIVAA assay was performed according to manufacturer's protocol (Trevigen). Briefly, 6-wk-old female nude mice were anesthetized with tribromoethanol (i.p., 250 mg/kg). A 1-cm incision was made on both dorsal-lateral surfaces of the animal and two basement membrane extract (BME)-filled angioreactors were implanted on each side. Each angioreactor contained a total of 25 μ L BME premixed with 20 μ g/mL heparin and 2 μ L of test conditioned medium or medium containing recombinant protein. Angioreactors were removed 11 d after implantation. The matrigel was digested with 300 μ L of CellSpere solution for 1 h (37 $^{\circ}$ C), and endothelial cells were labeled with FITC-lectin. Fluorescence was measured in 96-well plates (excitation 485 nm, emission 510 nm). Values for cell invasion are calculated as the ratio of relative fluorescent units (RFUs) of the test sample with respect to control sample.

Permeability Assays. HMVEC were seeded on collagen-coated transwells (3-mm-size pore, PTFE; Corning), transfected where corresponding, and allowed to grow as a 3-d-old mature monolayer. Following overnight starvation, 500 μ L and 100 μ L of test medium were added for 30 min (37 $^{\circ}$ C) to the bottom and top chamber, respectively. A total of 100 μ L of 1 mg/mL FITC-dextran (molecular weight = 40,000; Invitrogen) was added for 30 min. Fluorescence was quantified using a SpectraMax M5 Microplate Reader (Molecular Devices) with excitation at 494 nm and emission at 521 nm. For in vivo permeability assays, tumor-bearing mice received an i.v. injection of 100 μ L Evans blue dye. Thirty minutes later, the animals were killed and perfused with 0.5% paraformaldehyde solution through the left ventricle. Tumors were excised, dried (60 $^{\circ}$ C, 16 h), and weighed before Evans blue extraction in 1 mL of formamide at 55 $^{\circ}$ C for 16 h. Dye content was quantified at 610 nm in a spectrophotometer. For dextran retention, mice-bearing tumors received an i.v. injection of 100 μ L rhodamine-dextran (20 mg/mL in PBS; 400 kDa; Sigma). After 2 h, mice were killed and perfused. Tu-

mors were frozen and sections were processed for CD31 staining and analysis of vascular leakage using fluorescence microscopy.

Gene Expression Microarray. Total RNA from SVEC or vGPCR-expressing SVEC cells (four RNAs each) was extracted and transcribed to produce biotin-labeled cRNA using TrueLabeling-AMP Linear RNA Amplification Kit (SuperArray Biosciences). Labeled cRNA was purified using SuperArray ArrayGrade cRNA Cleanup Kit and quantified by spectrophotometry. Labeling efficiency was established by serial dilutions on nylon membrane with chemiluminescent detection. Gene expression

profiling was done using Oligo GEArray Mouse Angiogenesis Microarray (OMM-024; SuperArray Biosciences), which detects 113 key genes involved in angiogenesis. Prehybridization (2 h) and hybridization (overnight) was done in a hybridization oven (60 °C) using 6 µg of labeled cDNA target. High-stringency washing at 60 °C (0.1× SSC, 0.5% SDS) was followed by chemiluminescence detection. Array images were recorded using X-ray film and a flatbed desktop scanner to create grayscale (16-bit) files, then analyzed with the GEArray Expression Analysis Suite online software.

1. Montaner S, et al. (2003) Endothelial infection with KSHV genes in vivo reveals that vGPCR initiates Kaposi's sarcomagenesis and can promote the tumorigenic potential of viral latent genes. *Cancer Cell* 3:23–36.
2. Chiou CJ, et al. (2002) Patterns of gene expression and a transactivation function exhibited by the vGCR (ORF74) chemokine receptor protein of Kaposi's sarcoma-associated herpesvirus. *J Virol* 76:3421–39.
3. Montaner S, et al. (2006) The Kaposi's sarcoma-associated herpesvirus G protein-coupled receptor as a therapeutic target for the treatment of Kaposi's sarcoma. *Cancer Res* 66: 168–174.
4. Dourmishev LA, Dourmishev AL, Palmeri D, Schwartz RA, Lukac DM (2003) Molecular genetics of Kaposi's sarcoma-associated herpesvirus (human herpesvirus-8) epidemiology and pathogenesis. *Microbiol Mol Biol Rev* 67:175–212.

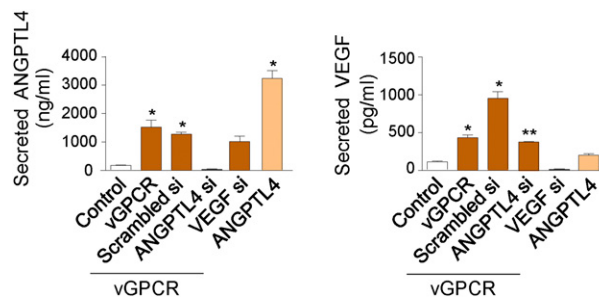


Fig. S1. Levels of VEGF and ANGPTL4 in conditioned media. HMEC1s were transfected with Scrambled (Scrambled si), ANGPTL4 (ANGPTL4 si), VEGF (VEGF si), or no siRNA and then with pCEFL Tet REV TA and pBIG AU5 vGPCR. Cells were left untreated (Control) or treated with (1 µg/mL) Dox (vGPCR). After 24 h, supernatants were collected. Supernatants of cells overexpressing ANGPTL4 (pcDNA3.1-ANGPTL4-mycHis; ANGPTL4) were also collected. Figure shows the corresponding levels of ANGPTL4 and VEGF in conditioned media, using ELISA, in a representative assay.

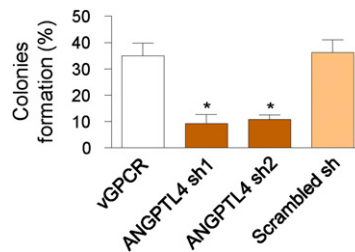


Fig. S2. In vitro proliferative capability in soft agar of ANGPTL4 sh lines. Two different clones were generated by stable transfection of ANGPTL4 shRNA in vGPCR-expressing SVECs (ANGPTL4 sh1 or sh2). The in vitro proliferative capability of these cell lines in soft agar, compared with the parental line (vGPCR), is shown.

Table S1. List of angiogenesis-related up-regulated genes in vGPCR-expressing SVEC cells (vGPCR) vs. control SVEC cells

Unigene	RefSeq RNA	Gene symbol	Gene name	Fold change
Mm.309336	NM_009640	<i>Angpt1</i>	Angiopoietin 1	1.12
Mm.435498	NM_007426	<i>Angpt2</i>	Angiopoietin 2	3.09
Mm.6645	NM_009652	<i>Akt1</i>	Thymoma viral proto-oncogene 1	1.32
Mm.196189	NM_020581	<i>Angptl4</i>	Angiopoietin-like 4	13.14
Mm.4487	NM_008486	<i>Anpep</i>	Alanyl (membrane) aminopeptidase	1.66
Mm.4352	NM_009929	<i>Col18a1</i>	Procollagen, type XVIII, α 1	2.92
Mm.389135	NM_007734	<i>Col4a3</i>	Procollagen, type IV, α 3	2.00
Mm.1238	NM_009971	<i>Csf3</i>	Colony stimulating factor 3 (granulocyte)	1.24
Mm.21013	NM_008176	<i>Cxcl1</i>	Chemokine (C-X-C motif) ligand 1	2.89
Mm.4979	NM_009140	<i>Cxcl2</i>	Chemokine (C-X-C motif) ligand 2	2.16
Mm.4660	NM_009141	<i>Cxcl5</i>	Chemokine (C-X-C motif) ligand 5	1.48
Mm.287977	NM_138302	<i>Ecgf1</i>	Endothelial cell growth factor 1 (platelet-derived)	1.19
Mm.982	NM_007901	<i>Edg1</i>	Endothelial differentiation sphingolipid GPCR1	1.02
Mm.331159	XM_892839	<i>Efna3</i>	Ephrin A3	2.89
Mm.209813	NM_010111	<i>Efnb2</i>	Ephrin B2	1.90
Mm.34533	NM_010144	<i>Ephb4</i>	Eph receptor B4	1.30
Mm.57094	NM_008006	<i>Fgf2</i>	Fibroblast growth factor 2	1.43
Mm.3403	XM_485825	<i>Fgf6</i>	Fibroblast growth factor 6	1.54
Mm.6904	NM_008010	<i>Fgfr3</i>	Fibroblast growth factor receptor 3	2.00
Mm.297978	NM_010216	<i>Figf</i>	C-fos induced growth factor	4.14
Mm.389712	NM_010228	<i>Flt1</i>	FMS-like tyrosine kinase 1	5.86
Mm.3879	NM_010431	<i>Hif1a</i>	Hypoxia inducible factor 1, α subunit	1.22
Mm.268521	NM_010512	<i>Igf1</i>	Insulin-like growth factor 1	3.17
Mm.874	NM_010548	<i>Il10</i>	Interleukin 10	1.82
Mm.103783	NM_008351	<i>Il12a</i>	Interleukin 12A	1.76
Mm.222830	NM_008361	<i>Il1b</i>	Interleukin 1 β	1.05
Mm.1019	NM_031168	<i>Il6</i>	Interleukin 6	3.44
Mm.227	NM_008402	<i>Itgav</i>	Integrin α V	1.07
Mm.277072	NM_008493	<i>Lep</i>	Leptin	2.89
Mm.4406	NM_013599	<i>Mmp9</i>	Matrix metalloproteinase 9	1.08
Mm.4627	NM_008727	<i>Npr1</i>	Natriuretic peptide receptor 1	1.41
Mm.266341	NM_010939	<i>Nrp2</i>	Neuropilin 2	1.67
Mm.432468	NM_153561	<i>Nudt6</i>	Nudix-type motif 6	1.08
Mm.144089	NM_011057	<i>Pdgfb</i>	Platelet derived growth factor, B polypeptide	2.13
Mm.971	NM_008877	<i>Plg</i>	Plasminogen	1.50
Mm.279690	NM_008973	<i>Ptn</i>	Pleiotrophin	1.16
Mm.86361	NM_021309	<i>Sh2d2a</i>	SH2 domain protein 2A	1.36
Mm.272920	NM_008541	<i>Smad5</i>	MAD homolog 5 (Drosophila)	2.59
Mm.20944	NM_025367	<i>Sphk1</i>	Sphingosine kinase 1	2.49
Mm.220821	NM_138672	<i>Stab1</i>	Stabilin 1	1.15
Mm.295194	NM_011532	<i>Tbx1</i>	T-box 1	1.76
Mm.275336	NM_011536	<i>Tbx4</i>	T-box 4	1.47
Mm.14313	NM_013690	<i>Tek</i>	Endothelial-specific receptor tyrosine kinase	5.73
Mm.137222	NM_031199	<i>Tgfa</i>	Transforming growth factor α	3.86
Mm.197552	NM_009370	<i>Tgfbr1</i>	Transforming growth factor, β receptor I	1.06
Mm.4159	NM_011580	<i>Thbs1</i>	Thrombospondin 1	2.27
Mm.26688	NM_011581	<i>Thbs2</i>	Thrombospondin 2	2.50
Mm.8245	NM_011593	<i>Timp1</i>	Tissue inhibitor of metalloproteinase 1	2.06
Mm.255332	NM_009396	<i>Tnfaip2</i>	Tumor necrosis factor, α -induced protein 2	1.39
Mm.344820	NM_011614	<i>Tnfsf12</i>	Tumor necrosis factor (ligand) superfamily, member 12	1.65
Mm.208152	NM_177371	<i>Tnfsf15</i>	Tumor necrosis factor (ligand) superfamily, member 15	3.92
Mm.358643	NM_011618	<i>Tnnt1</i>	Troponin T1, skeletal, slow	1.44
Mm.282184	NM_009505	<i>Vegfa</i>	Vascular endothelial growth factor A	1.60